The crystal structure of a third polymorph of $Cu_5(PO_4)_2(OH)_4$

GERALD L. SHOEMAKER, JAMES B. ANDERSON AND EDWARD KOSTINER[1]

Institute of Materials Science and Department of Chemistry
University of Connecticut
Storrs, Connecticut 06268

Abstract

A phase formed in the $CuO-P_2O_5-H_2O$ system is an additional polymorph of pseudo-malachite, $Cu_5(PO_4)_2(OH)_4$. This phase crystallizes in the space group $P\bar{1}$ with $a = 4.445(1)$, $b = 5.873(1)$, $c = 8.668(3)$Å, $\alpha = 103.62(2)$, $\beta = 90.35(2)$, $\gamma = 93.02(1)°$. The structure, solved by Patterson methods, was refined by full-matrix least-squares techniques to a residual $R = 0.022$ ($R_w = 0.036$). The four crystallographically unique copper atoms lie in characteristically distorted (four short and two long bonds) six-coordinated sites which link together to form two-dimensional copper-containing sheets. As in the other two polymorphs, these sheets (which are joined together by phosphate tetrahedra and hydrogen bonds) can be derived from a two-dimensional framework of edge-sharing, copper-containing polyhedra.

Introduction

The crystal structure of pseudomalachite (PM) was determined by Ghose (1963) and refined by Shoemaker *et al.* (1977). Recently, we described (Anderson *et al.*, 1977) the crystal structure of a synthetic polymorph of pseudomalachite which, as a convenience, we referred to as PPM.

During the course of a series of hydrothermal experiments designed to establish the conditions for equilibrium between PM and PPM, a careful visual inspection with a high-intensity light source revealed crystals which had a slightly bluer color than the surrounding products. X-ray powder diffraction examination revealed the presence of diffraction lines which could not be explained by the known polymorphs PM and PPM. A powder photograph of the blue-green material alone revealed it to be a third polymorph of $Cu_5(PO_4)_2(OH)_4$, which we shall call QPM.

This paper presents the results of our refinement of the structure of QPM and a description of its structure in terms of polyhedral linkages within a two-dimensional net. The following paper (Shoemaker and Kostiner, 1981) will present a more detailed summary of polymorphism among compounds of the stoichiometry $Cu_5(PO_4)_2(OH)_4$.

Experimental

Once the identity of the new phase had been established, it was found among the products of a number of previous experiments in hydrothermal copper phosphate systems. Additional experiments were carried out in an attempt to determine the effects of temperature and pressure variation on the increasingly complex equilibrium between the polymorphs of $Cu_5(PO_4)_2(OH)_4$.

QPM has never been obtained as the sole product of a hydrothermal reaction. Most commonly, it is found in close conjunction with PM, although in some experiments PPM was the only other polymorph observed. QPM has been grown by hydrothermal technique in sealed gold capsules from nutrient mixtures containing $Cu_3(PO_4)_2$, libethenite, malachite, or copper(II) nitrate with a variety of mineralizing solutions at pressures ranging from 1.2 to 4.0 kbar and bomb temperatures from 205 to 560°C. It has not been observed in mixtures whose pH after reaction was less than 6 or greater than 9.

The crystal used for data collection was obtained from the hydrothermal reaction between 67.4 mg $Cu_3(PO_4)_2$ and 0.5 ml of approximately 1.5 M K_3PO_4 solution held at 450°C and 3.8 kbar for four days. In this experiment, QPM formed dendritic crystals which were intimately mixed with PPM crystals and CuO. Significant amounts of QPM can be obtained by the

---

reaction of 77 mg libethenite with 103 mg K_2HPO_4 in 0.55 ml H_2O at slightly less than 300°C and 1.2 kbar for seven days. In the latter experiment twinned QPM crystals are obtained intermixed with PM and PPM only. In most runs where transport is observed, QPM (along with PM) favors the cooler end of the capsule.

The growth and spatial distribution of the polymorphs within the hydrothermal capsule are highly dependent upon the temperature of the experiment; little if any dependence upon pressure has been noted. The factors which govern the PM–PPM–QPM equilibria are still unclear. Along with temperature and pressure, the composition of the reaction mixture may control the products in a complex fashion (see Shoemaker and Kostiner, 1981).

QPM exhibits marked tendencies toward twinning and dendritic growth. No freely-growing single crystals have been observed. The material used for structural investigation was removed as a wedge-shaped tablet from between the arms of a dendritic formation of the same compound. An untwinned section of this block was carefully pre-shaped and ground to a sphere of average radius 0.19 mm. After orientation on the precession camera, the sphere was mounted on the Picker FACS-I diffractometer and centered for data collection.

The lattice parameters were determined in a PICK-II least-squares refinement program, using 24 reflections within the angular range $38° < 2\theta < 54°$; the re-

flections were automatically centered on a Picker FACS-I four-circle diffractometer using $MoK\alpha_1$ radiation ($\lambda = 0.70930Å$). At 22°C the lattice parameters are $a = 4.445(1)$, $b = 5.873(1)$, $c = 8.668(3)Å$, $\alpha = 103.62(2)$, $\beta = 90.35(2)$, $\gamma = 93.02(1)°$, where the figures in parentheses represent the standard deviations in the last reported figure. The calculated volume is $219.6Å^3$, giving a calculated density, with $Z = 1$, of 4.354 g cm^{-3}. Qualitative elemental analysis, performed by energy-dispersive X-ray fluorescence on the scanning electron microscope, indicated that copper and phosphorus were the only heavy elements present.

Diffraction intensities were measured using Zr-filtered $MoK\alpha$ radiation at a take-off angle of 1.5° with the diffractometer operating in the ω scan mode. Ten-second background counts were taken at both ends of a 1.4° θ–2θ offset corrected for dispersion. Of the 1432 independent data in the angular range $2\theta < 62°$, 1350 were considered observable according to the criterion $|F_o| > 3.0\sigma_F$, where σ_F is defined as $0.02|F_o| + [C + k^2B]^{1/2}/2|F_o|Lp$; the total scan count is C, k is the ratio of scanning time to the total background time, and B is the total background count. Three reflections were systematically monitored; the maximum variation in intensity observed was never greater than ±3% over the data collection period.

Intensity data were corrected for Lorentz and polarization effects, and absorption corrections ($\mu = 128$

Table 1. Fractional atomic coordinates and anisotropic thermal parameters*

Atom	10^4x	10^4y	10^4z	B_{11}	B_{22}	B_{33}	B_{12}	B_{13}	B_{23}
Cu(1)	0	1/2	1/2	0.81(2)	0.51(2)	0.99(2)	−0.05(1)	−0.43(1)	0.03(1)
Cu(2)	0	0	0	0.74(2)	0.53(2)	0.50(2)	−0.19(1)	−0.10(1)	0.20(1)
Cu(3)	0	1/2	0	0.88(2)	0.43(2)	1.12(2)	−0.06(1)	0.55(1)	0.14(1)
Cu(4)	343.4(8)	−301.2(6)	3289.4(4)	0.92(2)	0.80(1)	0.43(1)	−0.37(1)	0.03(1)	0.15(1)
P	5087(2)	3265(1)	2265.7(8)	0.43(2)	0.53(2)	0.53(2)	−0.07(2)	0.04(2)	0.10(2)
O(1)	6980(5)	3087(1)	767(3)	1.01(8)	0.85(7)	0.71(7)	−0.25(6)	0.34(6)	0.23(6)
O(2)	7054(5)	2946(4)	3657(3)	0.80(7)	0.88(7)	0.83(7)	−0.25(6)	−0.39(6)	0.25(6)
O(3)	2844(5)	1029(4)	1873(2)	0.78(7)	0.96(7)	0.60(7)	−0.47(6)	0.01(6)	0.15(6)
O(4)	6632(5)	4524(4)	7330(3)	1.00(8)	0.84(7)	1.65(9)	0.38(6)	0.13(7)	0.10(7)
O(5)	1695(4)	1955(3)	5272(2)	0.61(7)	0.70(7)	0.60(7)	−0.10(5)	−0.08(5)	0.23(5)
O(6)	1551(4)	2078(3)	8721(2)	0.55(7)	0.60(6)	0.55(7)	−0.06(5)	0.10(5)	0.15(5)

Numbers in parentheses are e.s.d.'s in the last significant figure.

The B's are defined by the general temperature factor

$$exp\left[-\tfrac{1}{4}(B_{11}h^2a^{*2} + B_{22}k^2b^{*2} + B_{33}l^2c^{*2} + 2B_{12}hka^*b^* + 2B_{13}hla^*c^* + 2B_{23}klb^*c^*)\right].$$

cm^{-1}, Mo$K\alpha$) were made using the program already cited. The maximum relative absorption correction was 5.6% of $|F_o|$.

An inspection of the unit-cell parameters and cell volume led to the suspicion that this material might be one of the polymorphs of PM and PPM which had been predicted during the structural investigation of these two compounds. Specifically:

PM	PPM	QPM
$a = 4.4728$Å	$c = 4.461$Å	$a = 4.445$Å
$V = 437.73$Å³	$V = 437.46$Å³	$V = 219.55$Å³
		$V \times 2 = 439.10$Å³

Therefore, the formula $Cu_5(PO_4)_2(OH)_4$ was used in initial structural trials and was confirmed in the final refinement.

The *b–c* plane of the Patterson map was carefully studied for vectors indicative of normal copper–copper distances. The copper positions determined in this manner were used to calculate a difference Fourier map from which the phosphorus and oxygen positions were determined in successive least-squares iterations. The positional parameters were refined using a full-matrix least-squares refinement (Busing *et al.*, 1962a), using a $1/\sigma^2$ weighting scheme, zerovalent scattering factors (Cromer and Mann, 1968), isotropic temperature factors, and corrections for secondary extinction and anomalous dispersion. The best isotropically refined parameters were placed into an anisotropic refinement which yielded a final residual, R, of 0.022 and a weighted residual R_w of 0.036. When a hydrogen atom was added near to O(5) (see below), the value of the residual R dropped to 0.021 ($R_w = 0.036$). Table 1 gives the final results of the anisotropic refinement; the structure factor data are presented in Table 2.[2] The maximum extinction correction (Zachariasen, 1968) was 30% of $|F_o|$ for the 100 reflection.

Results and discussion

The QPM structure contains four crystallographically distinct copper sites, one phosphorus site, and six oxygen sites. Cu(1), Cu(2), and Cu(3) lie on crystallographically independent inversion centers in characteristically elongated (4+2) octahedral sites at $(0, \frac{1}{2}, \frac{1}{2})$ $(0, 0, 0)$, and $(0, \frac{1}{2}, 0)$ respectively. The four closer oxygens lie in an approximately square planar arrangement at an average of 1.979Å for Cu(1) and

Table 3. Bond distances, angles, and polyhedral edge lengths for the copper polyhedra

		Distance (Å)	Angle (°)	Edge (Å)
Cu(1) polyhedron				
Cu(1)-O(2)	2x	1.918(2)		
Cu(1)-O(5)	2x	2.040(2)		
Cu(1)-O(4)	2x	2.578(3)		
O(2)-Cu(1)-O(5)			84.10(9)	2.653(3)
O(2)-Cu(1)-O(5)			95.90(9)	2.940(3)
O(2)-Cu(1)-O(4)			86.14(9)	3.108(3)
O(2)-Cu(1)-O(4)			93.86(9)	3.315(3)
O(5)-Cu(1)-O(4)			83.71(8)	3.108(3)
O(5)-Cu(1)-O(4)			96.29(8)	3.459(3)
Cu(2) polyhedron				
Cu(2)-O(6)	2x	1.936(2)		
Cu(2)-O(3)	2x	2.006(2)		
Cu(2)-O(1)	2x	2.287(2)		
O(6)-Cu(2)-O(3)			98.91(9)	2.998(3)
O(6)-Cu(2)-O(3)			81.09(9)	2.564(3)
O(6)-Cu(2)-O(1)			79.02(8)	2.701(3)
O(6)-Cu(2)-O(1)			100.98(8)	3.266(3)
O(3)-Cu(2)-O(1)			94.79(9)	3.167(3)
O(3)-Cu(2)-O(1)			85.21(9)	2.916(3)
Cu(3) polyhedron				
Cu(3)-O(1)	2x	1.925(2)		
Cu(3)-O(6)	2x	1.971(2)		
Cu(3)-O(4)	2x	2.700(3)		
O(1)-Cu(3)-O(6)			87.75(8)	2.701(3)
O(1)-Cu(3)-O(6)			92.25(8)	2.809(3)
O(1)-Cu(3)-O(4)			88.95(9)	3.287(3)
O(1)-Cu(3)-O(4)			91.05(9)	3.345(3)
O(6)-Cu(3)-O(4)			80.53(8)	3.070(3)
O(6)-Cu(3)-O(4)			99.47(8)	3.596(3)
Cu(4) polyhedron				
Cu(4)-O(3)		1.930(2)		
Cu(4)-O(5)		1.951(2)		
Cu(4)-O(6)		1.967(2)		
Cu(4)-O(5)		1.975(2)		
Cu(4)-O(2)		2.428(2)		
Cu(4)-O(4)		2.825(2)		
O(3)-Cu(4)-O(6)			82.29(9)	2.564(3)
O(3)-Cu(4)-O(5)			96.79(9)	2.920(3)
O(3)-Cu(4)-O(2)			91.19(9)	3.133(3)
O(3)-Cu(4)-O(4)			93.15(9)	3.508(3)
O(5)-Cu(4)-O(6)			98.79(9)	2.974(3)
O(5)-Cu(4)-O(5)			83.80(9)	2.622(4)
O(5)-Cu(4)-O(2)			97.15(8)	3.298(3)
O(5)-Cu(4)-O(4)			78.85(8)	3.108(3)
O(6)-Cu(4)-O(2)			95.53(8)	3.268(3)
O(6)-Cu(4)-O(4)			77.39(8)	3.070(3)
O(5)-Cu(4)-O(2)			73.29(8)	2.653(3)
O(5)-Cu(4)-O(4)			113.82(8)	4.048(3)

Numbers in parentheses are e.s.d.'s in the last significant figure.

1.972Å for Cu(2), but are significantly closer at 1.948Å for Cu(3). The two longer oxygens are at 2.578 and 2.287Å for Cu(1) and Cu(2), respectively, but are at 2.700Å for Cu(3). Cu(4) lies in a more distorted environment with four oxygens in an approximately square plane at an average distance of 1.956Å with O(2) completing a square pyramid at 2.428Å. O(4) lies opposite O(2) at 2.825Å and because of this extreme distance O(4) cannot be said to contribute significantly to Cu(4)'s primary coordination. However, the valence-deficient state of O(4) in the structural model suggests that the contribution from the Cu(4)–O(4) bond might be included even though it is small. The Cu(4) polyhedra may therefore be consid-

Table 4. Bond distances, angles, and polyhedral edge lengths for the phosphate tetrahedron

	Distance (Å)	Angle (°)	Edge (Å)
P-O(4)	1.513(2)		
P-O(1)	1.537(2)		
P-O(2)	1.539(2)		
P-O(3)	1.575(2)		
O(4)-P-O(1)		112.7(1)	2.539(3)
O(4)-P-O(2)		112.9(1)	2.544(3)
O(4)-P-O(3)		110.5(1)	2.537(3)
O(1)-P-O(2)		110.4(1)	2.526(3)
O(1)-P-O(3)		104.9(1)	2.466(3)
O(2)-P-O(3)		104.8(1)	2.467(3)

Numbers in parentheses are e.s.d.'s in the last significant figure.

Table 5. Bond distances, bond angles, and polyhedral edge lengths for oxygen polyhedra

	Distance (Å)	Angle (°)	Edge (Å)
O(1) polyhedron			
O(1)-P	1.537(2)		
O(1)-Cu(3)	1.925(2)		
O(1)-Cu(2)	2.287(2)		
P-O(1)-Cu(3)		137.2(1)	3.227(1)
P-O(1)-Cu(2)		119.1(1)	3.320(1)
Cu(3)-O(1)-Cu(2)		87.94(8)	2.9365(5)
O(2) polyhedron			
O(2)-P	1.539(2)		
O(2)-Cu(1)	1.918(2)		
O(2)-Cu(4)	2.428(2)		
P-O(2)-Cu(1)		132.0(1)	3.161(1)
P-O(2)-Cu(4)		120.1(1)	3.466(1)
Cu(1)-O(2)-Cu(4)		91.40(9)	3.1296(7)
O(3) polyhedron			
O(3)-P	1.575(2)		
O(3)-Cu(4)	1.930(2)		
O(3)-Cu(2)	2.008(2)		
P-O(3)-Cu(4)		129.1(1)	3.168(1)
P-O(3)-Cu(2)		127.5(1)	3.219(1)
Cu(4)-O(3)-Cu(2)		94.90(9)	2.902(1)
O(4) polyhedron			
O(4)-P	1.513(2)		
O(4)-Cu(1)	2.578(3)		
O(4)-Cu(3)	2.700(3)		
O(4)-Cu(4)	2.825(2)		
P-O(4)-Cu(1)		104.6(1)	3.306(1)
P-O(4)-Cu(3)		101.1(1)	3.340(1)
P-O(4)-Cu(4)		176.7(2)	4.336(2)
Cu(1)-O(4)-Cu(3)		110.34(2)	4.334(2)
Cu(1)-O(4)-Cu(4)		76.47(6)	3.4238(7)
Cu(3)-O(4)-Cu(4)		77.69(6)	3.466(1)
O(5) polyhedron			
O(5)-Cu(4)	1.951(2)		
O(5)-Cu(4)	1.975(2)		
O(5)-Cu(1)	2.040(2)		
Cu(4)-O(5)-Cu(4)		96.18(9)	2.922(1)
Cu(4)-O(5)-Cu(1)		118.1(1)	3.4238(7)
Cu(4)-O(5)-Cu(1)		102.43(9)	3.1296(7)
O(6) polyhedron			
O(6)-Cu(2)	1.936(2)		
O(6)-Cu(4)	1.967(2)		
O(6)-Cu(3)	1.971(2)		
Cu(2)-O(6)-Cu(4)		96.01(9)	2.902(1)
Cu(2)-O(6)-Cu(3)		97.41(9)	2.9365(5)
Cu(4)-O(6)-Cu(3)		123.3(1)	3.466(1)

Numbers in parentheses are e.s.d.'s in the last significant figure.
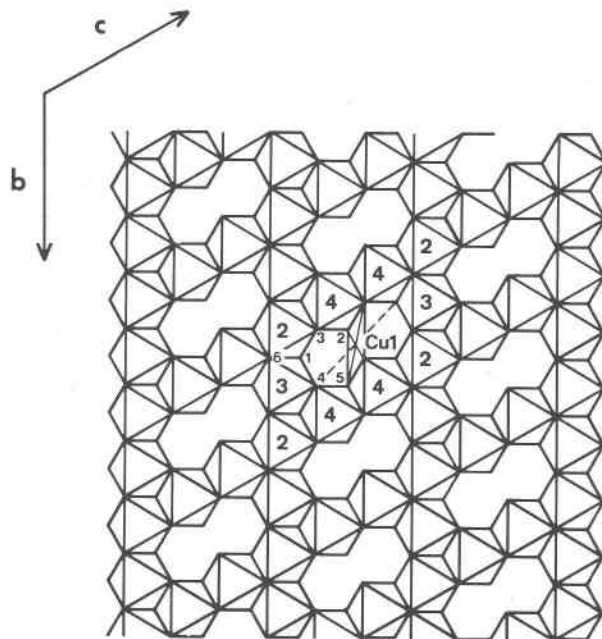
Fig. 1. The idealized two-dimensional framework of Cu(2), Cu(3), and Cu(4) octahedra (large numbers) found in QPM. The Cu(1) site is shown. Small numbers indicate oxygen atom positions.

ered as [4+1+(1)]. The bond distances and angles of the copper polyhedra are given in Table 3. The standard deviations for all bond lengths and angles were computed by the function and error program ORFFE (Busing et al., 1962b).

The phosphate tetrahedron is quite distorted with a short bond to O(4) of 1.513Å and a long bond to O(3) of 1.575Å, with a total average bond length of 1.541Å. The angles O(4)–P–O are all considerably greater than the ideal tetrahedral angle, ranging from 112.9 to 110.5° while the angles involving O(3)–P–O are considerably compressed with a minimum of 104.8°. The dimensions of the phosphate tetrahedra are given in Table 4.

With the exception of O(4) the oxygen atoms exhibit three-fold coordination by copper and phosphate atoms. O(1), O(2), and O(3) are all bonded to one phosphorus and two copper atoms and O(5) and O(6) are bonded to three copper atoms. Table 5 presents the bond distances and angles about the oxygen atoms.

Like its polymorphs, the structure of QPM is characterized by layers of edge-sharing copper polyhedra joined in the third dimension by phosphate tetrahedra. The phosphate tetrahedra share two oxygen atoms in one layer and two in the adjacent layer. The short unit-cell translation corresponds roughly to the distance between adjacent copper-containing layers.

The copper-containing layer is based on a two-dimensional, four-connected net which is formed from intersecting chains of edge-sharing copper polyhedra. There are two types of chains, each extending infinitely along a cell axis (Fig. 1). The first consists of alternating Cu(2) and Cu(3) octahedra which share opposite edges to form chains extending along the *b* axis. The second type consists of Cu(2) octahedra alternating with pairs of inversion-related, edge-sharing Cu(4) polyhedra to form chains extending along *c*. As implied, the two chains cross through the Cu(2) site, with all three polyhedra sharing a common vertex at O(6).

The Cu(1) site can be viewed as an unique site created within the holes of the four-connected net with the phosphates attaching near the ends of these holes. A projection of the four-connected net as it would be formed by perfect octahedra is shown in Figure 1, with the unique Cu(1) position indicated. This idealized net can be altered by rotating and distorting the octahedral sites to give the actual copper-containing layer of QPM as shown in Figure 2. The layers stack almost directly over one another so that the chains and holes of each layer nearly superimpose onto those of the next layer. The derivation of the idealized model and the relation of QPM to the other polymorphs will be discussed in the following paper (Shoemaker and Kostiner, 1981).

Bond length–bond strength calculations (Brown and Wu, 1976) for the oxygen atoms indicate that O(5) and O(6) are seriously valence-deficient at 1.26 and 1.37 valence units, respectively, when their bonds to three copper atoms alone are considered. O(5) and O(6) are the obvious choices for the O–H sites on the basis of this calculation and also from the fact that the geometry of their bonds to three copper
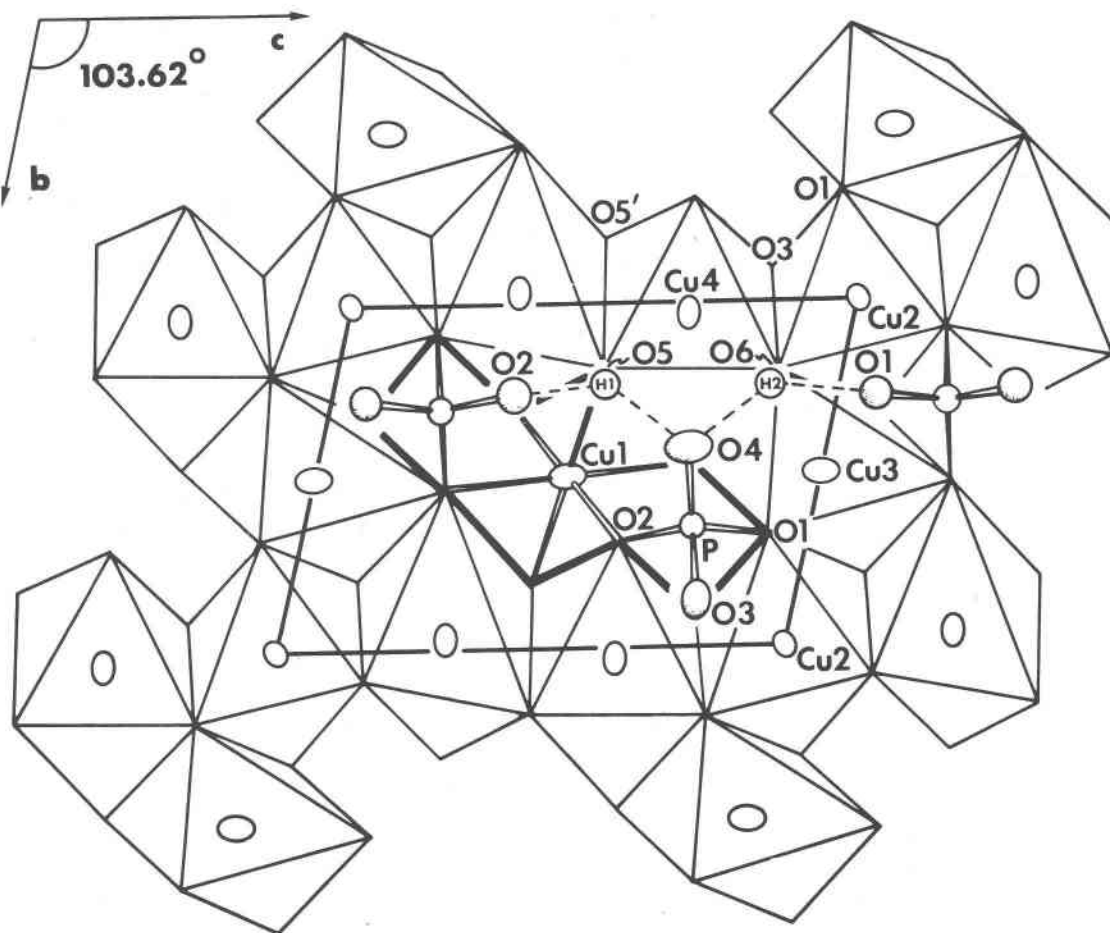
Fig. 2. A projection of the actual QPM layer onto the *bc* plane (down *a**). The Cu(2), Cu(3), and Cu(4) sites are illustrated as six-coordinated polyhedra to emphasize the relationship to the idealized framework shown in Fig. 1. Oxygen atoms lie at the polyhedral vertices except for those in the next layer out of the page. Possible H-acceptor bonds are drawn with dotted lines. The unit cell is outlined.

atoms allows the hydrogen to complete a tetrahedral distribution of cations around each oxygen.

When the final difference Fourier map was searched for peaks at the expected hydrogen positions, some candidate peaks were revealed. When the positions of these peaks were entered into final structural refinements, only one of them remained stable. The H(1) position was refined in a full-matrix, least-squares refinement with 96 variables and stabilized at 0.4389, 0.2449, 0.5445 (isotropic thermal parameter 2.7Å^2) at a distance of 1.218Å from O(5) [2.016Å from O(4) and 2.022Å from O(2)]. All of the possible H(2) locations failed to stabilized during structural refinement, indicating that the difference Fourier peaks are more strongly influenced by termination errors from the heavy copper atoms than by contributions from the lone hydrogen atoms.

The O(6) atom is the logical site for the second hydrogen atom. On the basis of several considerations, including the valence requirements of the associated oxygen atoms, H(2) was assigned an approximate po-

sition of 0.43, 0.26, 0.87, at a distance of 1.24Å from O(6) and 2.07 and 2.09Å from O(4) and O(1), respectively. The possible hydrogen atom locations are shown in Figures 2 and 3. Figure 3 shows that the hydrogens assume positions approximately midway between successive layers of copper atoms.

A valence sum analysis of the remaining oxygen atoms indicates that O(1) and O(2) are mildly valence-deficient at 1.95 and 1.90 v.u., respectively. However, O(4) is found to be significantly valence-deficient, having a sum of only 1.56 valence units when contributions from all three copper atoms and the phosphorus atom are considered. O(4) can only fulfill its valence requirements if it is allowed to accept a hydrogen bond contribution from both H(1) and H(2), which are primarily bonded to O(5) and O(6) respectively. Although Brown's paper (1976) on hydrogen bonding is primarily concerned with the results of neutron diffraction experiments, his Figure 1 affords a means of estimating the valence contribution from a weak hydrogen bond on the basis of the
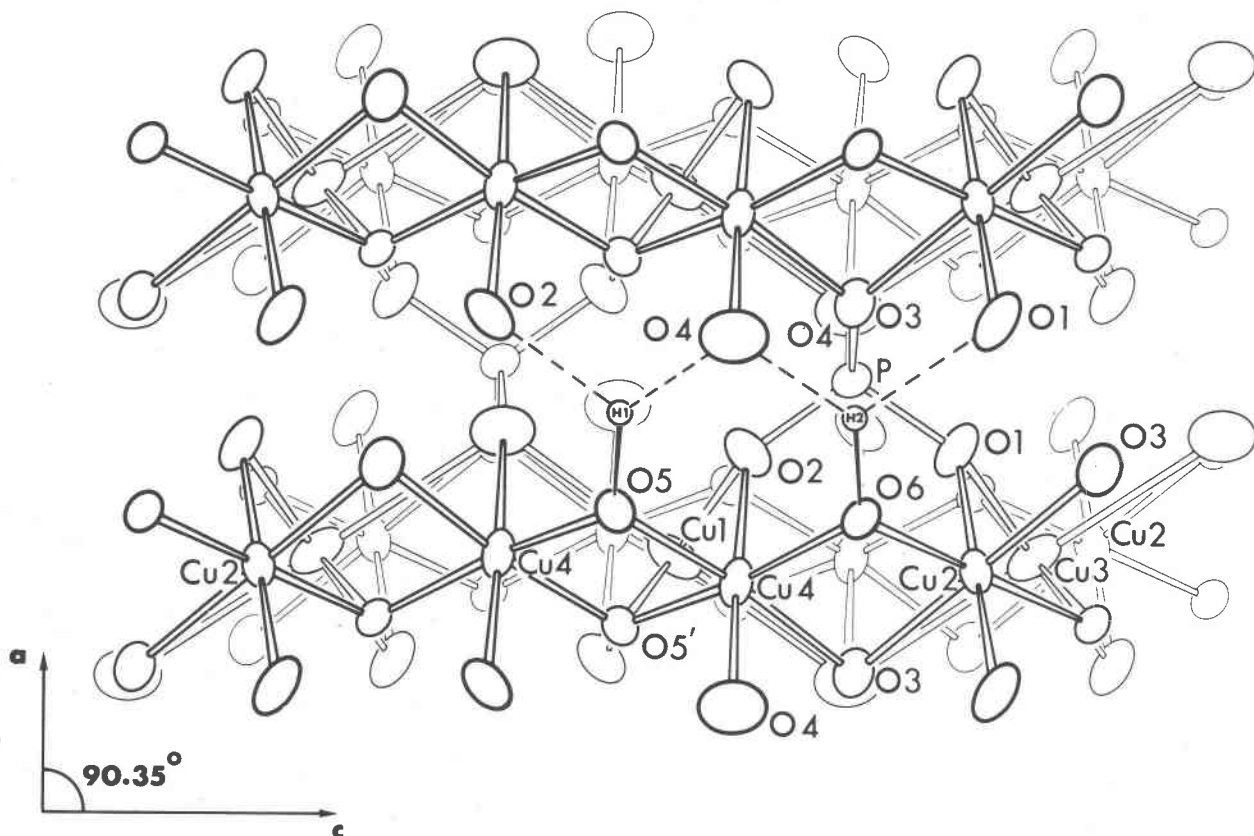
Fig. 3. A projection of the QPM structure down *b** onto the *ac* plane. The contents of one unit cell are shown. Possible H-acceptor bonds are drawn with dotted lines.

oxygen–oxygen distance alone. As a weak hydrogen bond acceptor, O(4) might be expected to receive approximately 0.1 v.u. each from bonds with H(1) [O(4)–O(5) = 2.935Å] and H(2) [O(4)–O(6) = 3.017Å]. Although this approximation leaves O(4) still considerably underbonded at about 1.8 v.u., it does indicate that O(4) may be receiving an important share of its valence requirements from H-acceptor bonds with both hydrogen atoms.

On the basis of interatomic distances alone, the O(1) and O(2) atoms might be expected to receive valence contributions of about the same magnitude from hydrogen acceptor bonds to H(2) and H(1) respectively [O(1)–O(6) = 2.936Å, O(2)–O(5) = 2.872Å]. Since the valence sum analysis indicates that the needs of O(1) and O(2) are not as great as those of O(4), it is unclear how the hydrogen bonds will be distributed between these atoms. Both H(1) and H(2) may be participating in bifurcated hydrogen bonds to their two oxygen neighbors. The positions of these bonds are indicated in Figures 2 and 3.

Acknowledgments

References

Anderson, J. B., Shoemaker, G. L., Kostiner, E., and Ruszala, F. A. (1977) The crystal structure of synthetic Cu$_5$(PO$_4$)$_2$(OH)$_4$, a polymorph of pseudomalachite. American Mineralogist, 62, 115–121.

Brown, I. D. (1976) On the geometry of O–H···O hydrogen bonds. Acta Crystallographica, A32, 24–31.

Brown, I. D. and Wu, K. K. (1976) Empirical parameters for calculating cation–oxygen valences. Acta Crystallographica, B32, 1957–1959.

Busing, W. R., Martin, K. O., and Levy, H. A. (1962a) ORFLS, a Fortran crystallographic least-squares refinement program. U.S. National Technical Information Service, ORNL-TM-305.

Busing, W. R., Martin, K. O., and Levy, H. A. (1962b) ORFFE, a Fortran crystallographic function and error program. U.S. National Technical Information Service, ORNL-TM-306.

Cromer, D. T. and Mann, J. D. (1968) X-ray scattering factors computed from numerical Hartree–Fock wave functions. Acta Crystallographica, A24, 321–324.

Ghose, S. (1963) The crystal structure of pseudomalachite, Cu$_5$(PO$_4$)$_2$(OH)$_4$. Acta Crystallographica, 16, 124–128.

Shoemaker, G. L., Anderson, J. B., and Kostiner, E. (1977) Refinement of the crystal structure of pseudomalachite. American Mineralogist, 62, 1042–1048.

Shoemaker, G. L. and Kostiner, E. (1981) Polymorphism in Cu$_5$(PO$_4$)$_2$(OH)$_4$. American Mineralogist, 66, 176–181.

Zachariasen, W. H. (1968) A general theory of X-ray diffraction in crystals. Acta Crystallographica, A23, 558–564.